Real-World Crash Reconstruction using Finite Element Modeling to Examine Traumatic Rupture of the Aorta

Chirag S. Shah, Muralikrishna Maddali, Sandip A. Mungikar, Philippe Beillas, Warren N. Hardy, and King H. Yang
Wayne State University, Bioengineering Center.

Paul G. Bedewi, and Kennerly Digges
FHWA/NHTSA National Crash Analysis Center, The George Washington University.

Jeffrey Augenstein
The William Lehman Injury Research Center, University of Miami School Of Medicine

Abstract

One of the leading causes of death in automotive crashes is traumatic rupture of the aorta (TRA) or blunt aortic injury (BAI). The risk of fatality is high if an aortic injury is not detected and treated promptly. The objective of this study is to investigate TRA mechanisms using finite element (FE) simulations of reconstructed real-world accidents involving aortic injury. For this application, a case was obtained from the William Lehman Injury Research Center (WLIRC), which is a Crash Injury Research and Engineering Network (CIREN) center. In this selected crash, the case vehicle was struck on the left side with a Principal Direction of Force (PDoF) of 290 degrees. The side structure of the case vehicle crushed a maximum of 0.33 m. The total delta-V was estimated to be 6.2 m/s. The occupant, a 62-year old mid-sized male, was fatally injured. The occupant sustained multiple rib fractures, laceration of the right ventricle, and TRA, among other injuries.

The method proposed in this study allowed simulation of a real-world accident. The method involved two phases. First, the car-to-car interaction was simulated using car FE models. The FE car models were obtained from the National Crash Analysis Center (NCAC) public model archives, and were modified to represent the actual crash vehicles. The simulation was validated against intrusion and crush data.

Second, the interaction between the occupant and the interior of the automobile was simulated using input as the results of the first simulation. The occupant was modeled using a whole-body human FE model developed at Wayne State University. The model was developed to simulate the human body response to impact and includes descriptions of all major thoracic and abdominal organs, major blood vessels including the aorta, and all major bony structures. The model represents a mid-sized male. The aortic stress patterns observed in the FE simulation were compared to the autopsy findings.

It is hoped that the predicted internal kinematics of the thorax can help to better understand the injury mechanism of TRA. Results can also be used to design future experimental studies aiming at producing TRA in cadavers.

Introduction

Blunt Aortic Injury (BAI) or Traumatic rupture of the Aorta (TRA) is the second most common cause of death associated with motor vehicle crashes (MVCs), following only traumatic brain injury (Sauaia et al. 1995). It has been estimated that approximately 7500 to 8000 people die because of BAI in the United States every year (Mattox 1989). According to Sailer (1942), the first reference to traumatic rupture of the thoracic aorta was made by Vesalius in 1557. Since then, both retrospective studies and laboratory experiments were carried out to investigate the mechanism of BAI. Despite this long history, the underlying mechanism of the BAI is still not very well understood.

In a retrospective study, McGwin et al. (2003) examined the 1995 to 2000 National Automotive Sampling System (NASS) data to evaluate the relationship between risk of BAI and selected occupant, vehicle, and collision characteristics. During these five years, 20,191 cases of BAI were identified among approximately 31 million occupants. Only 11.4 % of the BAI cases survived. 64.4% of the fatalities occurred at the accident scene. McGwin et al. (2003) found that BAI occurred predominantly in frontal and near-side impact, corresponding to 45% and 22.5% of the BAI cases respectively. They also found that high age, lack of seatbelt use, high delta-V, high crush and intrusion increased the risk of BAI.

While reviewing the 1995 to 2001 NASS data, Steps (2003) found that the rate of aortic injury was the highest in near-side impact scenarios: near side impacts represented only 15% of all vehicle-to-vehicle crashes but were responsible for 28% aortic injuries. Steps (2003) also concluded from a re-examination of cadaver test data that V*C (viscous criteria) was the best predictor among the group of predictors she considered, and that door with soft padding might reduce injury risk to the aorta. From an analysis of real world crashes she found that delta-V and age significantly increased the risk of aortic injury.

In another study, Burkhart et al. (2001) reported 242 cases (12.4%) of aortic injury out of 1,957 autopsies performed after traumatic deaths in Marion County (Indiana) from 1984 to 1997. Of these 242 BAI cases, 165 (68%) resulted from MVCs. Of all these MVCs, 45% crashes were head on collisions and 35% were lateral crashes. Only 58% of the victims had the classic isthmus laceration suggesting that nonisthmus and complex aortic laceration were not uncommon in fatal BAI.

Dosios et al. (2000) reported similar findings from 11,446 medicolegal autopsies performed over a 3-year period (1994-1996) at the Athens Forensic Medicine Service. They recorded 12.7 % cases (251 victims) with blunt or penetrating aortic injury. A majority of aortic injury cases (72.8%) resulted from high speed MVCs. The remaining aortic injuries were due to falls, and compression by heavy machinery, blocks or stones.

Several laboratory experiments were also conducted on animal and/or human cadaver subjects. Coermann et al. (1972) used accelerating sled in their head on collision experiments on six unembalmed human cadavers. The objectives of their study were to produce aortic injury at classic isthmus location and to demonstrate the effectiveness of energy absorbing steering wheel assembly in preventing thoracic injuries. Aortic ruptures were produced in two experiments with smaller hub diameter and less energy absorbing steering wheel. Out of these two, one was at classic isthmus location. It was believed that the sternum was forced back against the spine and the inflexion of the sternum shoveled

mediastinal soft tissues toward the upper thoracic aperture. This mechanism was originally proposed by Voigt and Wilfert (1969) and became known as the "Voigt's Shoveling" effect.

In frontal impact experiments by Kroell et al. (1974), 23 unembalmed human cadavers were subjected to midsternal impact using either a mass of 19.5 kg or 23.1 kg and speeds ranging from 4.0 m/s to 10.0 m/s. The impact was delivered through a wooden form of diameter 150 mm with edge radius 12 mm. Prior to testing, the aorta was pressurized using a saline solution. Only two aortic injuries were generated even though the pressure measured within the aorta was as high as 210 kPa.

In another study reported by Viano (1989), 14 unembalmed human cadavers were subjected to a total of forty-four blunt lateral impacts to the chest and abdomen. The impacts were delivered using a 150 mm diameter and 23.4 kg pendulum launched at nominal speeds of 4.5, 6.7 or 9.4 m/s. The prime objective of this study was to develop response corridors for the chest and abdomen of the human cadavers subjected to blunt impact. No aortic injury was reported even though the impactor speed was as high as 9.4 m/s in some chest impacts.

In another cadaveric study, Cavanaugh et al. (1990, 1993) were able to produce five aortic tears among a total of seventeen tests performed using a horizontally accelerated sled and a Heidelberg-type seat fixture at speeds of about 9 m/s. It was hypothesized that the inertial forces exerted by laterally accelerating heart and vessels might have pulled on the descending thoracic aorta, which was firmly anchored to the posterior chest wall. This might have caused aortic tears near the junction between the aortic arch and the descending thoracic aorta.

Nusholtz et al. (1985) carried out experiments on live anesthetized canine using 10 kg hydraulic ram at speeds up to 14 m/s. They were able to produce aortic injuries at the aorta-heart junction, and at the junctions between the aorta and its superior branches. It was concluded that aortic trauma was only possible if subjects were frontally impacted above the sternum, causing compression of the chest followed by downward motion of the heart.

Shatsky et al. (1974) observed TRA after impacting primate chest with a pendulum at a speed of 5 m/s. Using flash X-ray cinematography, they observed high compression of the intra-thoracic organs. They believed that the entrapment of the aorta between heart and spine was the probable cause of aortic tears.

In experiments by Hanson (1967), five beagle dogs were subjected to superior-inferior (±Gz) deceleration and. Radiography was made during the test to observe the motion of thoracic visceral contents. It was concluded that tension due to the inertial effect of the heart and diaphragm on the ascending and descending aorta was responsible for aortic tear just distal to the left subclavian artery. Letterer (1924) also believed that downward traction of the heart due to fall was responsible for the aortic root avulsion. Others believed that rapid anterior-posterior deceleration caused differential forces between various organs and were responsible for the aortic injury (Hass 1944; Zehnder 1960; Newman and Rastogi 1984).

Several other injury mechanisms for the BAI were also reported in the literature. Squeezing of the aorta by the parietal pleura was proposed by Marshall (1958). Rindfleisch (1893) proposed stretch deformation of the aorta. Moffat et al. (1966) believed that the recurrent laryngeal nerve could contribute to aortic injury. Crass et al.

(1990) proposed the theory of osseous pinch, which suggested that circumferential tears could be caused by impingement of the great vessel by the upper ribs. Some suggested that TRA was two-times more likely in the presence of upper rib and sternum fracture (Dischinger et al. 1988), while others suggest that the incidence was the same in the presence of both upper and lower rib fractures (Kirshner et al. 1983), and with or without sternum fractures (Sturm et al. 1989). Klotz and Simpson (1932) and Oppenheim (1918) focused on increased intravascular pressure to be responsible for the TRA. This increased pressure could lead to an explosive outburst of the vessel. Lundevall (1964) proposed "water hammer" effect might be responsible for aortic rupture.

As a summary, laboratory experiments have yielded limited success in producing aortic injury. Retrospective studies have established a statistical link between BAI and various crash parameters (including delta-V, crush, intrusion, direction and type of impact, restrain system, age, sex, etc.), which could predict internal thoracic response. Various interpretations of those studies have led researchers to propose a variety of possible injury mechanisms for the BAI. However, there is no consensus regarding the mechanisms actually involved in BAI resulting from MVCs. This makes it difficult in development of an injury criteria aimed at preventing BAI. While existing injury criteria for the thoracic region may help to mitigate the overall injury risk, they do not specifically target internal organ injuries such as the BAI.

Therefore, it is critical to further improve the understanding of the underlying injury mechanism of BAI during crashes. This may require, the *in-vivo* response of the intra-thoracic organs including the aorta. However, knowing the interaction between organs during a real-world crash where instrumentation is not possible. As an alternative approach, we propose use of finite element (FE) computer models to reconstruct real-world MVCs that involved aortic injury to the occupant. It is hoped that this will help design future experimental studies and improve the understanding of BAI.

The objective of the current study was to demonstrate the feasibility of this approach. Finite Element vehicle models and a whole-body human FE model were employed to reconstruct a real-world crash where an occupant suffered fatal aortic injury. Simulations of the car-to-car impact and of the interaction of the occupant with the interior of the struck vehicle were conducted successfully.

Methods

Real-world crash: case selection and details

The real-world aortic injury case was obtained from the William Lehman Injury Research Center (WLIRC), which is a Crash Injury Research and Engineering Network (CIREN) center. Several considerations were given at the time of selecting case from the available cases in the WLIRC database. The case selected for current study had a delta-V of approximately 6.2 m/s (14 MPH) and structural damage to the case vehicle was relatively limited. The occupant of the case vehicle was 62 year old male with 1.73 m (68 in) height and 79 kg (174 lbs) weight, which is close to a 50^{th} percentile male as described by Schneider et al. (1983). The selected real-world case involved a 1990 Lexus ES-250 (case vehicle) and a 1983 Oldsmobile Cutlass (principal other vehicle, POV). The case vehicle was equipped with manual 3-point lap and shoulder belt and driver-side airbag. During the crash, the occupant was wearing the belt and the airbag deployed.

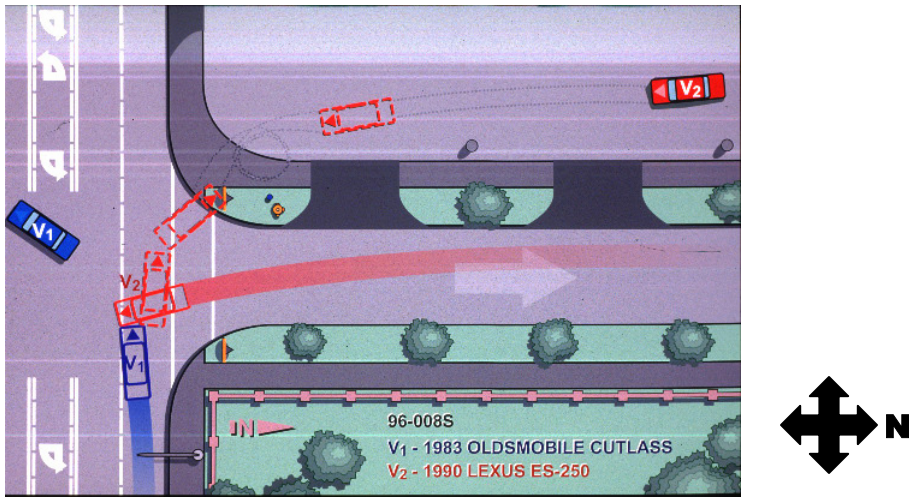

Figure 1: Accident scene diagram (***Courtesy***: William Lehman Injury Research Center (WLIRC))

The crash occurred at a 3 legged intersection, with a main road oriented east-west direction and a one way secondary road north of the main road.

The POV was traveling west on the main road. The case vehicle was traveling south on the secondary road, driving in wrong way. The driver of the case vehicle entered the intersection and attempted to make a left turn (direction east). The case vehicle drove directly across the path of the POV and was struck on the left side by the front of the POV. The driver of the POV saw the case vehicle coming from his right and attempted to avoid a collision by steering to the left. Direct damage on the case vehicle started 2.92 m (115 in) forward of the left rear axle. The direct damage extended rearwards a total of 1.96 m (77 in). The direction of force was estimated 10 o'clock (CDC code: 10-LYAW-3). The side structure was crushed to a maximum depth of 0.33 m (13 in).

After the impact with the POV, the case vehicle rotated clockwise. The POV rotated counterclockwise and the two vehicles impacted in a side slap collision. The POV continued to rotate counterclockwise and came to rest facing south-west. The case vehicle continued forward in a northwest direction. It mounted the northwest curb of the intersection, crossed the grass, struck the 'One Way' street sign and continued to rotate clockwise. It stopped rotating facing south and rolled rearwards to a block wall located at the rear of a gas station lot, where it finally stopped.

The POV was not available for evaluation. As a result, the missing vehicle algorithm of the SMASH (Simulating Motor Vehicle Accident Speeds on the Highway) program was used to calculate the delta-V for the case vehicle. SMASH computed a lateral component of the delta-V at 6.2 m/s, which was found same as the total delta-V.

Simulation setup

The selected real-world crash was numerically reconstructed in two phases.

1. Car-to-car crash numerical reconstruction (Phase 1). A sub-model including the driver-side structures of the case vehicle was defined and its kinematics was saved for Phase 2.

2. A whole-body human FE model added to the sub-model of Phase 1 in order to simulate the interaction of the occupant with the interior of the case vehicle (Phase 2).

Phase-1: Car-to-car crash numerical reconstruction

Two FE vehicle models were obtained from the National Crash Analysis Center (NCAC) public FE model archive. The Ford Taurus side impact FE model was used to represent the case vehicle (1990 Lexus ES-250) and the Ford Taurus frontal impact FE model was used to represent the POV (1983 Oldsmobile Cutlass). The Taurus has dimensions that are similar to those of the two vehicles involved in the crash. The two models were converted from the LS-Dyna (LSTC, Livermore, CA) fixed format to the LS-Dyna keyword format. The unit system was changed from millimeter, second and metric tonne to millimeter, millisecond and kilogram to make it consistent with the whole-body human FE model. Masses were adjusted to the match the mass of the actual vehicles by adding lumped mass at the center of gravity of FE vehicle models (Table 1). The masses of the occupants were simulated by adding masses to the nodes of the driver seats (Table 1). These two FE models were then combined in one file for the simulation. The two vehicles models were initially positioned as in the real crash data. This step required rotation and translations of both FE vehicle models.

Table-1: Real crash vehicle and FE vehicle model details

	Case vehicle	POV
Real crash	1990 Lexus ES-250	1983 Oldsmobile Cutlass
FE reconstruction	Ford Taurus (side impact model)	Ford Taurus (frontal impact model)
Gross vehicle weight (kgs)	1457.78	1544
Occupant weight (kgs)	77.3 (driver)	76.5 (driver)

The model was then setup for the impact. This included the construction of a fixed rigid plane to simulate the ground, the definition of contacts between vehicle models as well as contacts between vehicle models and the ground. The Ford Taurus side impact model was kept stationary while the Ford Taurus frontal impact model was given an initial velocity of 6.2 m/s (14 mph), which was the delta-V estimated for the real crash. A general contact, covering large portions of the vehicle models, was defined (Figure 2). The total simulation time was 200 milliseconds. For the model of the case vehicle, the driver side structures including the front and rear doorframe, door armrest and left B-Pillar nodes, were grouped and their motions were recorded in a separate binary file (referred to as “interface file” in the LS-Dyna manuals) to be used for the Phase 2 simulation. Those structures will be referred to as “door structure” hereafter.

Structural deformation patterns obtained in the simulation were compared with the real crash data using the final animation of the simulation and the photograph of the real vehicle after the crash. Intrusion and crush obtained from the simulation were compared with the real crash data for CDC (Collision Deformation Classification) measurements. The simulation was repeated, tuning the impact angle and position of the POV model until a reasonable match was obtained for the case vehicle data. A series of simulations were conducted with varying impact angles ranging from 210 to 330 degrees.

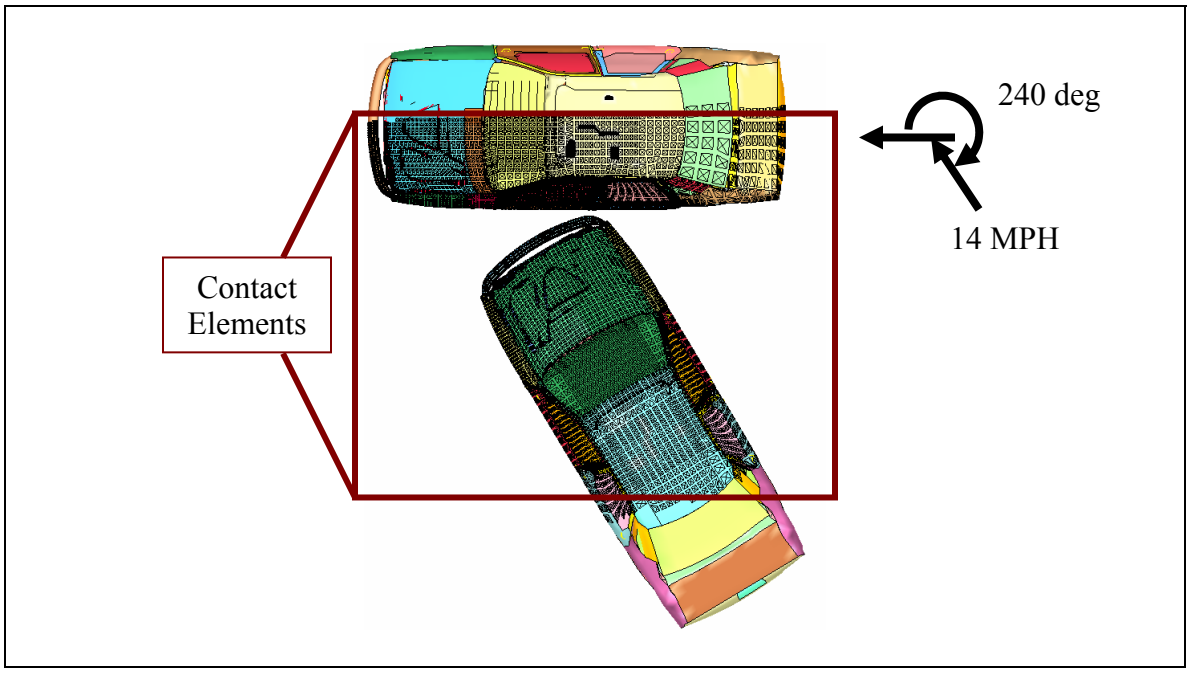

Figure 2: Phase-1 simulation setup.

Phase-2: Sub-modeled case vehicle model door structure-to-whole-body human FE model simulation

The whole-body human FE model required for this phase simulation was developed at Wayne State University by integrating three component FE models. The integration is detailed in Shah et al. (2004). The model includes a detailed description of the main bony structures, organs, and soft tissues of the human shoulder, thorax and abdomen (Figure 3(a)). In the trunk region (Figure 3(b)), the model includes the main organs and vessels. The aorta, vena cava, lungs, heart, spleen, liver, kidneys, pleura, intercostals muscles, shoulder ligaments, shoulder muscles and their associated tendons are modeled using deformable elements. Three body-bags (airbags) represent the hollow abdominal organs such as gall bladder, urinary bladder, pancreas, small and large intestine. The organs are surrounded by the rib cage and spine, which are also modeled with deformable elements.

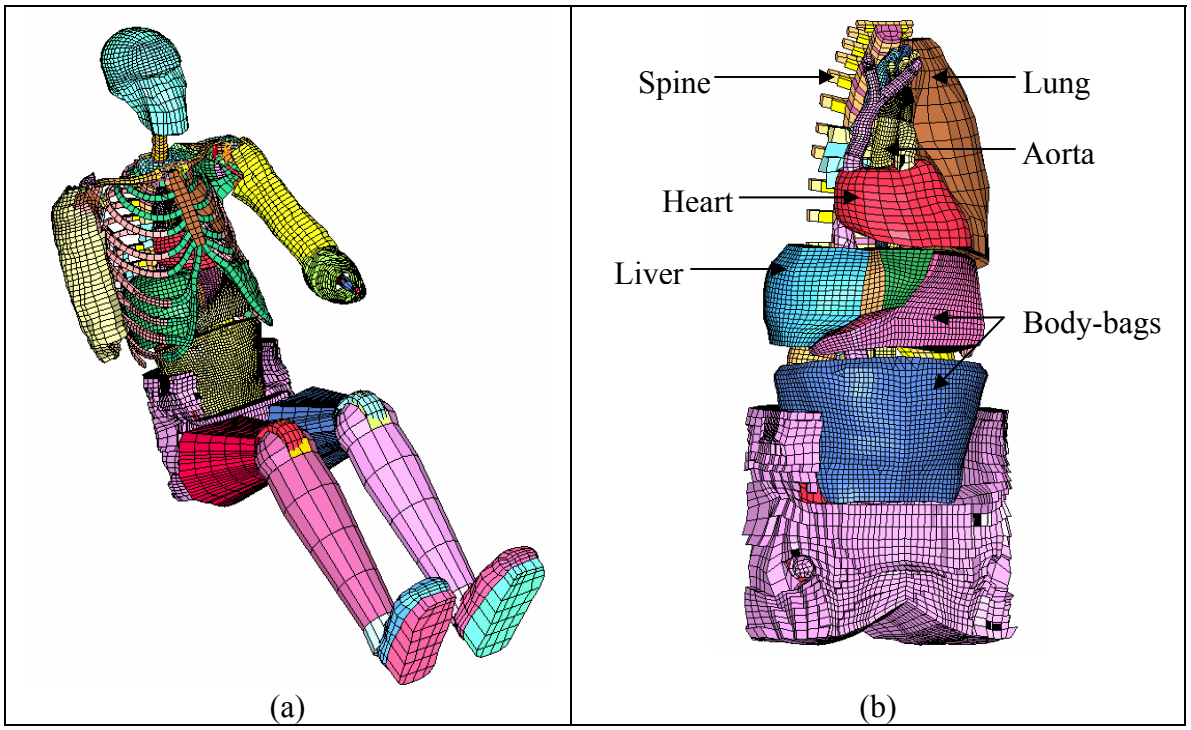

Figure 3: The whole-body human FE model (Shah et al. 2004).

The whole-body human FE model was imported into the case vehicle model and was positioned in a seated posture. The seating posture was determined based on post-crash photographs of the interior structures and seat. The door structure of the case vehicle model and the whole-body model were exported to a new LS-Dyna input file, removing the rest of the vehicles. The new model, referred to as the "sub-model" hereafter, is shown in Figure 4.

This sub-model was then setup for the Phase-2 simulation. A contact interface was created between the door structure and the occupant. The nodal motion of the door structure (previously saved in the interface file) was applied to the sub-model. The simulation was run for 80 milliseconds. Principal stresses predicted in the aorta model were compared with occupant's autopsy findings.

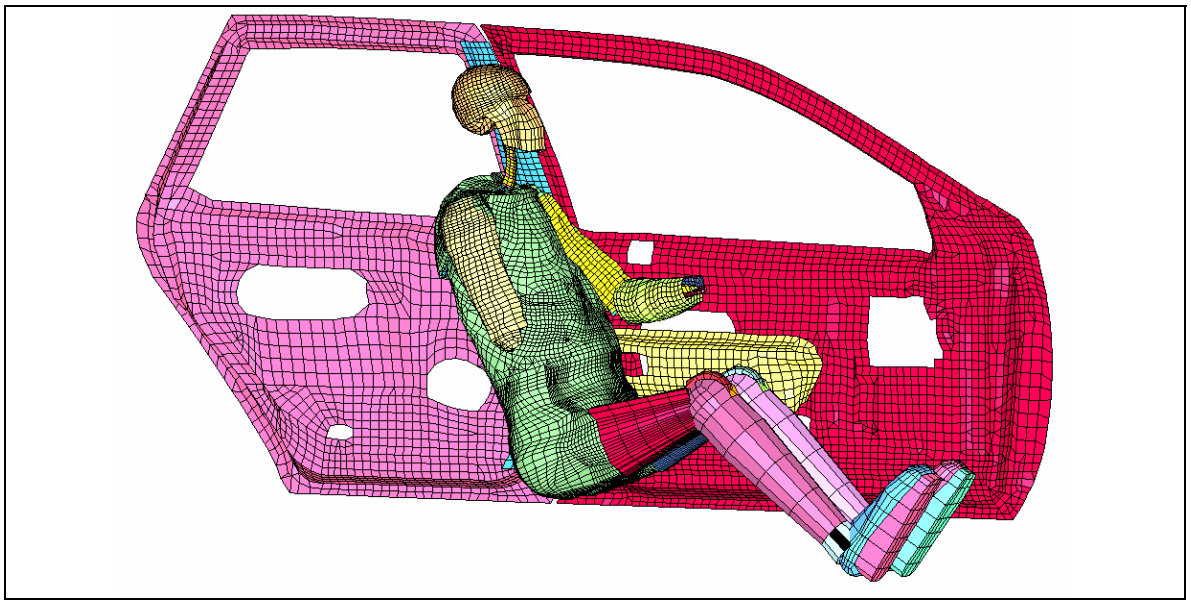

Figure 4: The door substructure and the whole-body human FE model in seating posture for Phase-2 simulation.

Results

Phase 1 simulation

For the Phase-1 simulation, the best match in terms of structural deformation was obtained for a 240-degree angle of impact. Figure 5 shows schematic representation of the Phase 1 simulation setup at the time of impact and at the end of the simulation. This angle is different from the 290 degrees (10 'O' clock) direction predicted by the CDC and the SMASH program. The reason for this mismatch is not clear.

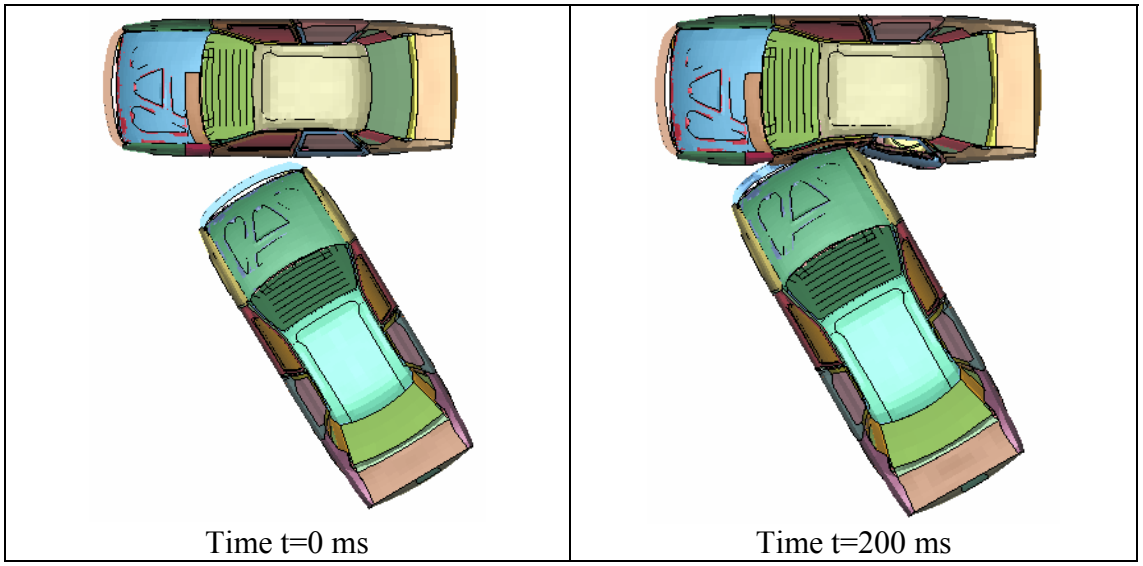

Figure 5: Phase-1 simulation results at the start and at the end of simulation.

Figure 6 compares deformation pattern of the FE case vehicle with real crash vehicle. The comparison revealed reasonable match between both the real crash and FE simulation.

(***Courtesy***: William Lehman Injury Research Center (WLIRC))

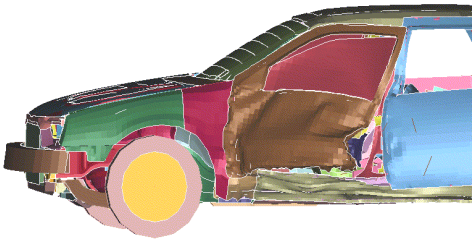

Figure 6: Deformation comparison between the real case vehicle and the FE vehicle model for Phase-1 simulation.

Quantitative comparisons of intrusion and crush deformation data between real-world crash and computer simulation were performed at three locations. The deformation data for the FE simulation were obtained from nodal time histories. The simulation results were within 15% of the real crash data (Table 2), which is considered a reasonable match.

Table-2 Comparison of deformation data for real crash and FE simulation

	Real crash deformation (mm)	Simulation results of Phase 1	
		FE Deformation (mm)	Node ID
B-pillar intrusion	140	131	31350
Left front door intrusion	210	241	41689
Left front door crush	330	303	38811

Phase 2 simulation

Figure 7 shows the interaction of the whole-body human FE model with the door structure. During the simulation it was found that the B-pillar and the armrest of the door structure engaged the shoulder, and the abdomen of the whole-body human FE model respectively. The state of maximum intrusion for the door was reached approximately 80 ms after the impact (Figure 7b).

During the real crash, the occupant sustained major laceration of the descending thoracic aorta, right ventricle laceration, multiple ribcage fractures among other injuries. As the material properties used in the current occupant model do not simulate failure, it is not possible to compare directly the rupture in the model with the injuries. Quantitative comparison is not possible either as there was no quantitative occupant data available from the real crash. For illustration purposes only, the stress contour within the aorta was plotted and is displayed in Figure 8. The objective here was not to determine if failure

could occur but only to visualize which part of the aorta was subjected to the highest stresses. It appears that the maximum stresses were reached in the descending aorta. It is interesting to notice that this was also the location where a major laceration was found during the autopsy. However, at this point, no conclusion should be drawn on the models capabilities to predict injury considering the current modeling limitations.

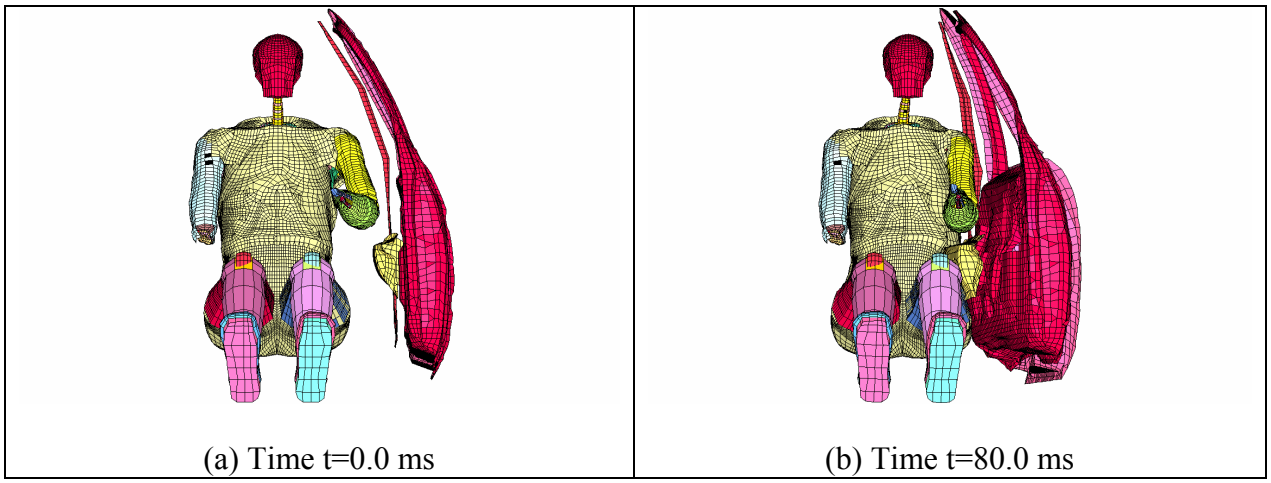

(a) Time t=0.0 ms (b) Time t=80.0 ms

Figure 7: Interaction of the whole-body human FE model and the door structure for the Phase-2 simulation prior to impact and at the state of maximum door intrusion.

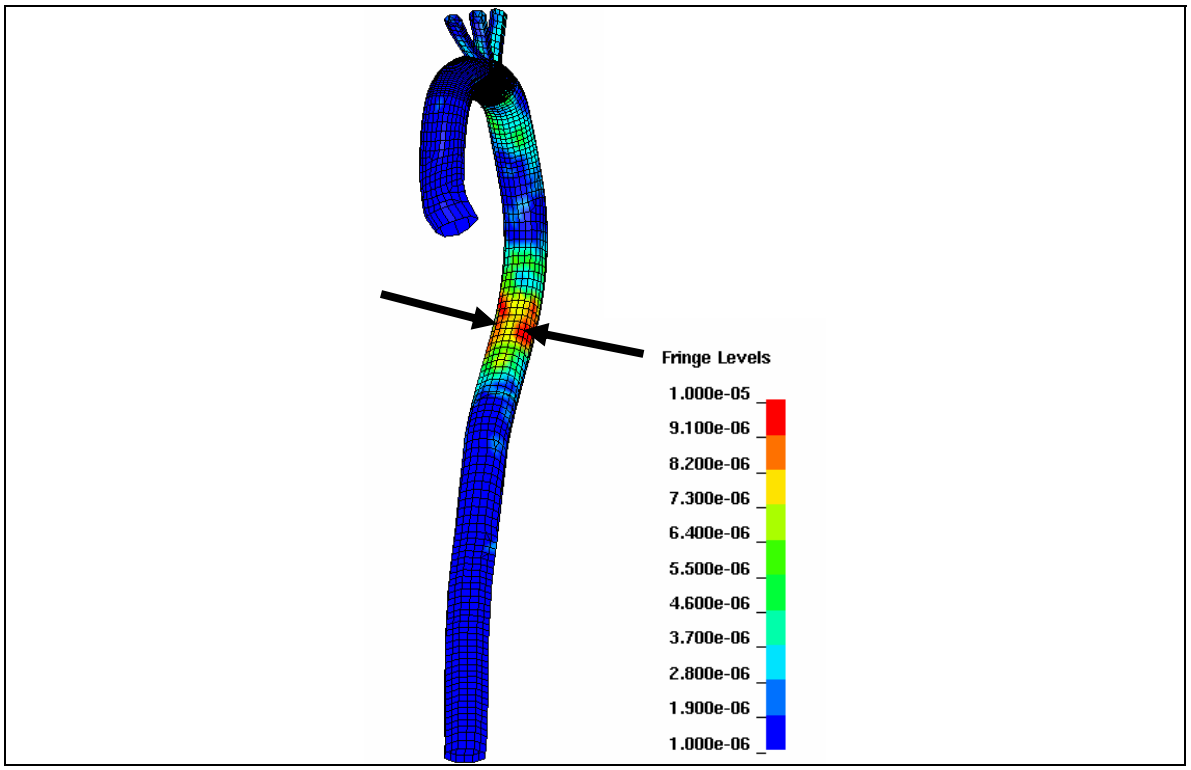

Figure 8: Location of the maximum stress in the aorta during the simulation. The maximum stresses were located in the descending aorta and are displayed with arrows. Stress contours represent the first principal stresses.

Discussion and Conclusions

The method used allowed simulation of a car-to-car impact, and then put a model of an occupant in conditions reflective of the real crash. Reasonable agreement was attained between the model predictions and the data available from the real crash. We believe that this demonstrates the feasibility of the approach. However there are still significant limitations that need to be addressed before the method can be used to reliably investigate aortic injury mechanisms.

First, there are limitations due the lack of data documenting the real crash. In particular, the car deformation was only available at three locations and the delta-V of the real case was estimated using incomplete data (the speed estimate of the bullet vehicle was not available). No quantitative data were available for the occupant. While it is not expected that quantitative data about the occupant response during the crash will be available in the future, more information about the seating posture may be of focus for future studies and simulations. In the current study, the seating posture was based on rough estimates derived from available photographs. It is unknown how much effect the seating posture would have on the occupant response. A sensitivity analysis focusing on seating and positioning parameters may be conducted in the future.

Second, there are still significant limitations in the car and occupant models. For the current study, the car models (Ford Taurus) were of the same class as the real vehicles but were of different make and models. The masses and overall dimensions of the vehicles models were adjusted to those of the real crash vehicles. But the geometric and structural differences between real world crash vehicles and FE vehicles were not adjusted. This can be improved only if large variety of vehicle models of the same class will be available to use for simulations.

It was also found that the occupant of the case vehicle was using available 3-point restrain system and that the airbag deployed during the real crash. For simplification purpose, the current study excluded seatbelt, airbag and seat from simulation, assuming that these restrains had minimal effect on occupant kinematics during the side impact. Future models may include those restraints in the simulation.

Finally, the whole-body human FE model was validated globally at the component level for a variety of impact scenarios (Shah et al. 2001; Lee and Yang 2001; Iwamoto et al. 2000). Local validation of the internal organs was not carried out due to lack of available biomechanical data. The whole-body human FE model is not able to simulate rib fracture and rupture of other tissues. The model is currently being modified to include those parameters for future studies. While this study can be considered as a significant step and has encouraging results, further improvements will be required before the approach can help improving the understanding injury mechanisms of BAI.

Acknowledgements

This study in part is funded by the George Washington University. The authors would also like to thank Jessica Steps, and George Bahouth (WLIRC, University of Miami) for helping in making the case details available.

References

Burkhart HM, Gomez GA, Jacobson LE, Pless JE, and Broadie TA. Fatal Blunt Aortic Injuries: A Review of 242 Autopsy Cases. J Trauma. 2001; 50:113-115.

Cavanaugh JM, Walilko TJ, Malhotra A, Zhu Y, and King AI. Biomechanical Response and Injury Tolerance of the Thorax in Twelve Sled Side Impacts. 34th Stapp Car Crash Conference. 1990; pp. 23-38. SAE Paper No. 902307.

Cavanaugh JM, Zhu Y, Huang Y, and King AI. Injury and Response of the Thorax in Side Impact Cadaveric Tests. 37th Stapp Car Crash Conference. 1993; pp. 199-221. SAE Paper No. 933127.

Coermann R, Dotzauer G, Lange W, and Voigt GE. The effects of the design of the steering assembly and the instrument panel on injuries (especially aortic rupture) sustained by car drivers in head-on collision. J Trauma. 1972; 12(8):715-724.

Crass JR, Cohen AM, Motta AO, Tomashefski JF. Jr, and Wiesen EJ. A proposed new mechanism of traumatic aortic rupture: the osseous pinch. Radiology. 1990; 176(3):645-649.

Dischinger PC, Cowley RA, Shanker BS, and Smialek JE. The incidence of ruptured aorta among vehicular fatalities. Proc. 32nd Association for the Advancement of Automotive Medicine Conference. 1988; pp. 15-23.

Dosios TJ, Salemis N, Angouras D, and Nonas E. Blunt and Penetrating Trauma of the Thoracic Aorta and Aortic Arch Branches: An Autopsy Study. J Trauma. 2000; 49:696-703.

Hanson PG. Cardiac displacement and thoracic vascular injury resulting from abrupt deceleration of dogs. Aerospce Medicine. 1967; 38:1259-1263.

Hass GM. Types of internal injuries of personnel involved in aircraft accidents. Journal of Aviation Medicine. 1944; 15:77-84.

Iwamoto M, Miki K, Mohammad M, Nayef A, Yang KH, Begeman PC, and King AI. Development of a Finite Element Model of the Human Shoulder. Stapp Car Crash Journal. 2000; 44:281-297.

Kirshner R, Seltzer S, D'Orsi C, and DeWeese JA. Upper rib fractures and mediastinal widening: indications for aortography. Annals of Thoracic Surgery. 1983; 35(4):450-454.

Klotz O, and Simpson W. Spontaneous Rupture of the Aorta. American Journal of Medical Science. 1932; 184:455-473.

Kroell CK, Schneider DC, and Nahum AM. Impact Tolerance and Response of the Human Thorax II. Proc. 18th Stapp Car Crash Conference. 1974; SAE Paper No. 741187.

Lee JB, and Yang KH. Development of a finite element model of the human abdomen. Stapp Car Crash Journal. 2001; 45:79-100.

Letterer E. Beitrage zur entstehung der aortenruptur an typischer stele. Virch. Arch. Path. Anat. 1924; 253:534-544.

Lundevall J. The Mechanism of Traumatic Rupture of the Aorta. Acta Path. Microbiol. Scand. 1964; 62:34-46.

Marshall TK. Traumatic dissecting aneurysms. Journal of Clinical Pathology. 1958; II:36-38.

Mattox KL. Fact and fiction about management of aortic transaction. Ann Thorac Surg. 1989; 48:1-2.

McGwin G, Metzger J, Moran SG, and Rue LW. Occupant- and Collision-Related Risk Factors for Blunt Thoracic Aorta Injury. J. Trauma. 2003; 54:655-662.

Moffat RC, Roberts VL, and Berkas EM. Blunt trauma to the thorax: development of pseudo-aneurysms in the dog. Journal of Trauma. 1966; 6:666-680.

Newman RJ, and Rastogi S. Rupture of the thoracic aorta and its relationship to road traffic accident characteristics. Injury. 1984; 15:296-299.

Nusholtz GS, Kaiker PS, Bosio AC, and Kirsh M. Thoracis Response to Frontal Impact. Proc. 29th Stapp Car Crash Conference. 1985; pp. 17-48. SAE Paper No. 851721.

Oppenheim F. Gibt es eine spontanrupter der gesunden aorta und wie kommt sie zustande. Münchener Medizinische Wochenschrift. 1918; 65:1234-1237.

Rindfleisch E. Zur entstehung and heilung des aneurysma dissecans aortae. Virch. Arch. Path. Anat. 1893; 131:374-378.

Sailer S. Disecting aneurysm of the aorta. Arch Pathol. 1942; 33:704-730.

Sauaia A, Moore FA, Moore EE, et al. Epidemiology of trauma deaths: a reassessment. J. Trauma. 1995; 38:185-193.

Schneider LW, Robbins DH, Pflug MA, and Snyder RG. Anthropometry of Motor Vehicle Occupants. Vol. 2. 1983. UMTRI-83-53-2. NHTSA.

Shah CS, Lee JB, Hardy WN, and Yang KH. A Partially Validated Finite Element Whole-Body Human Model for Organ Level Injury Prediction. Proceedings of IMECE04. 2004 ASME International Mechanical Engineering Congress. 2004 (In press).

Shah CS, Yang KH, Hardy WN, Wang KH, and King AI. Development of a computer model to predict aortic rupture due to impact loading. Stapp Car Crash Journal. 2001; 45:161-182.

Shatsky SA, Alter WA III, Evans DE, Armbrustmacher V, Earle KM, and Clark G. Traumatic distortions of the primate head and chest: Correlation of bimechanical, radiological and pathological data. Proc. 18th Stapp Car Crash Conference. 1974; pp. 351-381. SAE Paper No. 741186.

Steps J. Crash Characteristics Indicative of Aortic Injury in Near Side Vehicle-to-Vehicle Crashes. Ph.D. Dissertation. The George Washington University. 2003.

Sturm JT, Luxenberg MG, Moudry BM, and Perry JF. Does sternal fracture increase the risk for aortic rupture? Annals of Thoracic Surgery. 1989; 48:697-698.

Viano DC. Biomechanical Responses and Injuries in Blunt Lateral Impact. Proc. 33rd Stapp Car Crash Conference. 1989; pp. 113-142. SAE Paper No. 892432.

Voigt GE, and Wilfert K. Mechanisms of injuries to unrestrained drivers in head-on collisions. Proc. 13th Stapp Car Crash Conference. 1969; pp. 295-313. SAE Paper No. 690811.

Zehnder MA. Accident Mechanism and Accident Mechanics of the Aortic Rupture in the closed Thorax Trauma. Thoraxchirurgie und Vasculaere Chirurgie. 1960;8:47-65.